

## Recurrence spike spectra

**K. Hauke Kraemer · Frank Hellmann · Jürgen Kurths · Norbert Marwan**

Received: date / Accepted: date

**Abstract** A novel kind of power spectrum is constructed, the *inter spike spectrum*, which transforms any signal into its spike-frequency domain. This method clearly shows the apparent cycles in the data and overcomes the problems for spike-train-like signals when using the obvious idea of Fourier-transforming it. We invent this instructive approach with the idea of transforming the  $\tau$ -recurrence rate of a recurrence plot (RP), which often has a spiky appearance. The  $\tau$ -recurrence rate is the density of recurrence points along diagonals of the RP, which are parallel to the main diagonal with a distance of  $\tau$ . In this context the inter spike spectrum can be interpreted as a nonlinear power spectrum of a potentially high dimensional system which constitutes the RP. The proposed measure is robust to noise and is able to detect and analyze bifurcations.

**Keywords** Bifurcations · Recurrence Analysis · Decomposition · Frequency Analysis

**PACS** 05.45.Tp, 05.90.+m, 89.90.+n, 02.70.Uu, 05.10.Ln, 05.45.-a, 05.45.Ac

### 1 Introduction

Recurrence Plots (RPs) provide a vivid representation of complex dynamics stemming from potentially high dimensional systems, Eq. (1).

$$R_{i,j}(\varepsilon) = \Theta(\varepsilon - \| \vec{x}_i - \vec{x}_j \|), \quad \vec{x} \in \mathbb{R}^d, \quad i, j \in [1, \dots, N]. \quad (1)$$

The simple idea to track recurring states of the  $d$ -dimensional trajectory  $\vec{x}_i$  of the system under study not only allows for a beneficial visualization of the dynamics, but also for its quantification, using certain structures in the RP, such as diagonal or vertical lines [12].

---

K. Hauke Kraemer · Jürgen Kurths · Norbert Marwan · Frank Hellmann  
Potsdam Institute for Climate Impact Research, Member of the Leibniz Association, 14473 Potsdam, Germany  
E-mail: hkraemer@pik-potsdam.de

K. Hauke Kraemer · Jürgen Kurths  
Institute of Physics and Astronomy, University of Potsdam, 14476 Potsdam, Germany

Norbert Marwan  
Institute of Geosciences, University of Potsdam, 14476 Potsdam, Germany

Jürgen Kurths  
Institute of Physics, Humboldt Universität zu Berlin, 12489 Berlin, Germany

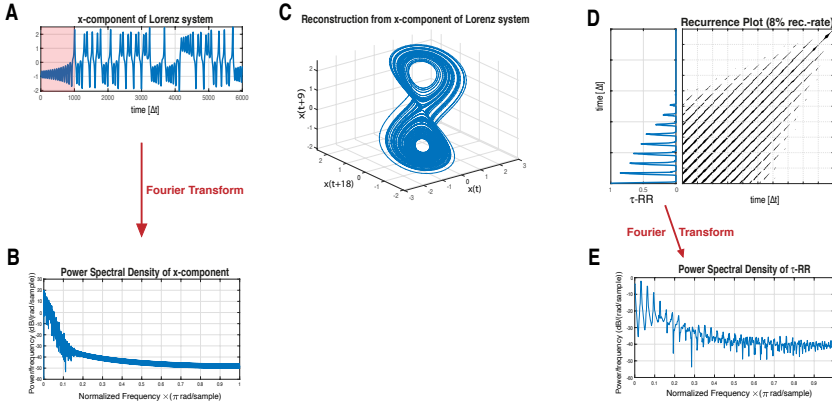


**Fig. 1** Schematic illustration of a  $\tau$ -recurrence rate based spectrum. **A**  $x$ -component time series of the Lorenz63-System (Eq. (8)) and **B** its corresponding Fourier power spectrum. **C** Reconstructed state space portrait from the time series shown in **A** using PECUZAL time-delay embedding [7]. **D** Subset of the recurrence plot and the corresponding  $\tau$ -recurrence rate obtained from the state space trajectory in **C**. The shaded interval in the time series in **A** corresponds to the shown subset. **E** Fourier Power spectrum obtained from the  $\tau$ -recurrence (subset shown in panel **D**) [19].

Some of these recurrence quantification measures, the entropy of diagonal lines and the entropy of recurrence times, can be related to the Kolmogorov-Sinai entropy [10, 1]. However, these quantifiers have a free parameter, the minimal considered line length, and are usually biased, due to the finite size of the RP and thickened diagonal lines, which needs to be corrected [6]. Moreover, the mentioned statistics cannot account for changing regular (non-chaotic) dynamics, such as period-doubling bifurcations. A rather simple idea is to look at the  $\tau$ -recurrence rate of the RP ( $\tau$ -RR, Eq. 2) [11, 19]. This is the density of recurrence points along the diagonals of the recurrence matrix, as a function of the distance  $\tau$  (sampling units) to the main diagonal:

$$\tau\text{-RR}(\varepsilon) = RR(\tau, \varepsilon) = \frac{1}{N - \tau} \sum_{i=1}^{N-\tau} R_{i,i+\tau}. \quad (2)$$

$\tau$ -RR serves as an estimator for the probability that the system recurs after time  $\tau\Delta t$ , with  $\Delta t$  being the sampling time of the trajectory  $\vec{x}_i = \vec{x}(\Delta t \cdot i)$ ,  $i = 1, \dots, N$ . Zbilut and Marwan [19] pointed out that  $\tau$ -RR could be used as a plugin value for the auto-correlation function  $C(\tau)$  and, hence, via the Wiener-Khinchim theorem a “generalized” powerspectrum can be obtained. This is reasonable, since the average distances for a given lag  $\tau$

$$\bar{D}(\tau) = \frac{1}{N - \tau} \sum_{i=1}^{N-\tau} D_{i,i+\tau} \quad (3)$$

can be directly read from the distance matrix **D** and is also preserved in its thresholded version  $\tau$ -RR. There are clear advantages for a recurrence-derived powerspectrum, i.e., Fourier transforming (FT)  $\tau$ -RR (Fig. 1D), instead of  $C(\tau)$  (Fig. 1C): There are no assumptions for stationarity or sampling, when constructing a RP. Furthermore, the correlation structures of higher dimensional spaces can be resolved in the recurrence-derived Fourier-spectrum.

However, there is a drawback to this approach. Whenever  $\tau$ -RR is a spike-train-like signal, which it is in most cases (see Fig. 1) especially for map-data (low-resolution data), a

FT of such a signal leads to a spike-train-like image in the frequency domain (e.g. [15, 4], see Fig. 1D). Thus, it is not intuitive how to extract meaningful information about dominant frequencies of the systems' state space trajectory.

For clarification, consider the signal we would like to analyze (e.g. the  $\tau$ -RR of a system) to be a Dirac comb (DC) with inter-spike period  $T_{is}$ :

$$DC_{is}(t) = \sum_{k=-\infty}^{\infty} \delta(t - kT_{is}), \quad (4)$$

i.e., a series of Dirac delta functions for a period  $T_{is}$ . There is only one single period –  $T_{is}$  – in this signal (Fig. 2A, D), so in principle we would strive for a single peak in the frequency domain of this signal at a frequency  $f = 1/T_{is}$ . Surprisingly the Fourier spectrum does not meet this expectation and instead of a single frequency, there are exceptionally many frequencies excited (Fig. 2B, E). This is, because the Fourier components add constructively for every frequency  $1/T_{is}$  and therefore  $DC_{is}(t)$  coincides with its own Fourier transform up to a factor  $1/T_{is}$ .

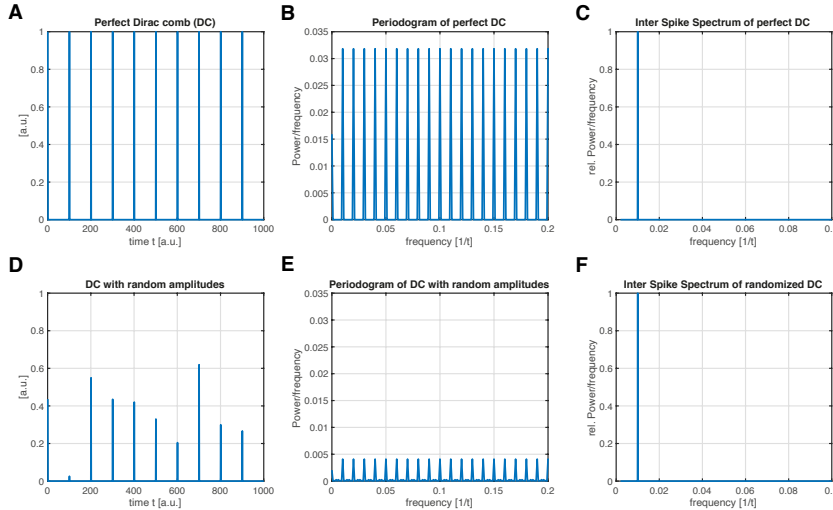


**Fig. 2** The transformation of a Dirac comb (series of Dirac delta functions) with a single inter-spike period  $T_{is} = 100$  ( $\hat{f} = 0.01$ ) into the frequency domain. **A** Dirac Comb (DC) with equal amplitudes and **B** its FFT-based powerspectrum. **C** Proposed inter spike spectrum of the signal in **A** showing a single frequency, which corresponds to the inter-spike period  $T_{is}$  ( $f = 0.01$ ). **D** DC with randomly chosen amplitudes and same  $T_{is}$  as in **A**, and **E** its FFT-based powerspectrum. **F** Proposed inter spike spectrum of the signal in **D** showing a single frequency, which corresponds to the expected inter-spike period  $T_{is}$  ( $f = 0.01$ ). Inter spike spectra were obtained with a LASSO regression and a regularization threshold corresponding to  $\rho = 0.9$  accordance of the signals in **(A,D)** and its re-composed signals (c.f. Section 2).

In this article we propose a new way of transforming a spike-train-like signal into its frequency domain. This novel *inter spike spectrum* does not show resonance behavior of the signal's inherent inter-spike frequencies (Fig. 2C, F). Section 2 explains the idea, which can be used to decompose any arbitrary signal and is not restricted to the  $\tau$ -RR, which we exemplify here. However, the more spiky the signal is, the more outstanding our new

approach is compared to a FT. In Section 3 we exemplify its use when transforming the  $\tau$ -RR of a system under study. In this case, the inter spike spectrum can unravel characteristic time scales of high dimensional systems, which is not possible when using a FT.

## 2 Method

The signal, which we would like to transform – we focus on  $\tau$ -RR in this article, but this can be applied to any sort of signal – is decomposed into a set of appropriate basis functions. Instead of using trigonometric functions, as it is the idea in the Fourier decomposition, we use Dirac combs (DC) with different inter-spike periods as basis functions, Eq. (4). Let  $s(t_i)$  be the normalized signal we want to transform with length  $N$  and  $t_i = i \cdot \Delta t$ ,  $i = 1, \dots, N$ , where  $\Delta t$  denotes the sampling time and  $s(t_i) \in [0, 1] \forall i$ . In the following we label this time series as a  $(1 \times N)$ -dimensional vector  $\mathbf{s}$ . First,  $\tilde{N}$  different DC's of length  $N$  are constructed with inter-spike periods  $T_{is} \in [1, \dots, \tilde{N}]$  and  $\tilde{N} = \lceil N/2 \rceil + 1$ . Second, in order to account for possible phase shifts of these basis functions occurring in  $\mathbf{s}$ , each of these  $\tilde{N}$  different DC's also need to be shifted one step further  $T_{is} - 1$  times. This leaves us with a total number of  $M = \sum_{i=1}^{\tilde{N}} i$  basis functions which we can arrange as rows of a  $(M \times N)$ -sized matrix  $\mathbf{X}$  (Fig. 3A illustrates the described procedure)

$$\mathbf{X}_{i,j} = \sum_{k=0}^N \delta(j - 1 - kT(i) - i + T(i)), \quad i = 1, \dots, \lceil N/2 \rceil + 1, \quad j = 1, \dots, N \quad (5)$$

$$T(i) = n, \quad \forall n : \frac{n(n-1)}{2} + 1 \leq i < \frac{n(n+1)}{2} + 1, \quad n \in \mathbb{N}_+. \quad (6)$$

Note that due to the shifting of each of the basis functions of inter-spike period  $T_{is}$ ,  $\mathbf{X}$  is not linear independent anymore. Furthermore, there will be identical basis functions and also basis functions, which do not allow for a unambiguous inter spike period, if we would include all  $N$  possible inter spike periods for a signal of length  $N$  instead of  $\lceil N/2 \rceil + 1$  (Fig. 3A). The reason is that in contrast to a trigonometric decomposition, where the Nyquist frequency marks a lower bound for the corresponding wave period, here the maximum considered inter spike period is bounded by  $T_{is}^{\max} = \lceil N/2 \rceil + 1$  (schematically illustrated in Fig. 3B).

Eventually, an under-determined linear system

$$\mathbf{X}^T \beta = \mathbf{s} \quad (7)$$

has to be solved for  $\beta$ , a  $(M \times 1)$ -sized vector carrying the loadings we are interested in. Along a variety of algorithms which can solve this problem, we are particularly interested in those solutions, which promote sparsity in  $\beta$ , since our goal is to decompose the signal  $\mathbf{s}$  into a minimal number of basis functions (for an excellent overview of the topic we refer to Brunton and Kutz [2]). In this paper we either use the *least absolute shrinkage and selection operator* (LASSO) [18] or a *sequentially thresholded least squares* (STLS) regression [3, 2] to obtain a solution  $\hat{\beta}$ . Finally, we group loadings which correspond to basis functions having the same period  $T_{is}$  into  $\hat{\beta}_f$  and obtain the *inter spike spectrum* by simply plotting  $\hat{\beta}_f$  as a function of the frequency  $f = T_{is}^{-1}$ , with  $T_{is} = \Delta t, 2\Delta t, \dots, (\lceil N/2 \rceil + 1)\Delta t$  (Fig. 2C, F).

In addition to the computational complexity of solving Eq. (7), the proposed method must also deal with the free choice of the regression regularization parameter  $\alpha$ , which determines the sparsity of the regression coefficient vector  $\beta$ . Obviously, there will be numerous peaks in the inter spike spectrum of a given signal, when  $\alpha$  is small, since  $\alpha = 0$

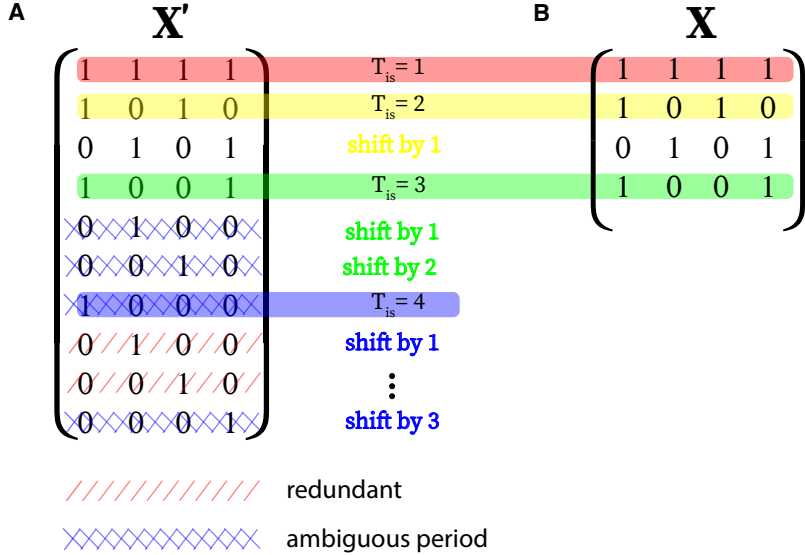


**Fig. 3** **A** Example for a full set of basis functions for an input signal of length  $N = 4$ , aligned in the matrix  $\mathbf{X}'$ . Inter spike periods  $T_{is}$  larger than  $[N/2] + 1$  lead to redundant basis functions (i.e., repeated lines in  $\mathbf{X}$ , red sheared) or basis functions, which can not be uniquely assigned to a certain inter spike period (blue sheared). **B** The final set of unambiguous, but still linearly dependent, basis functions aligned in the matrix  $\mathbf{X}$ .

corresponds to the least squares solution and the corresponding  $\hat{\beta}$  is an exact solution of Eq. 7 and not sparse. On the other hand, only a sparse number of non-zero loadings in  $\hat{\beta}$  – aka peaks in the inter spike spectrum – are obtained when  $\alpha$  is sufficiently large. In this paper we select  $\alpha$  such that the re-composed signal  $\tilde{s} = \mathbf{X}^T \hat{\beta}$  matches a given (Pearson) correlation coefficient  $\rho$  between the original signal  $s$  and itself.

### 3 Application

We exemplify the use of the inter spike spectrum in combination with the  $\tau$ -RR as outlined in Section 1 on several interesting research questions. The procedure is the following:

- (1) Compute a RP of the trajectory of the system, Eq. (1).
- (2) Compute the  $\tau$ -RR of that RP, Eq. (2).
- (3) Transform the  $\tau$ -RR into the proposed inter spike spectrum, see Section 2.

#### 3.1 Period estimation for different dynamics in the Rössler system

First, we consider the Rössler system (Eq. (9) in Appendix B.2) in three different dynamical setups. We use the proposed inter spike spectrum to identify the type of dynamics. We set the parameters  $b = 2$ ,  $c = 4$  and analyze period-2 limit cycle dynamics ( $a = 0.36$ , Fig. 4A, D, G, J), period-3 limit cycle dynamics ( $a = 0.41$ , Fig. 4B, E, H, K) and chaotic dynamics ( $a = 0.428$ , Fig. 4C, F, I, L).

The inter spike spectra unravel the specific dynamics, which are also apparent in the state space portraits (Fig. 4A, B, C) and in the  $\tau$ -RRs (Fig. 4G, H, I). The proposed idea is

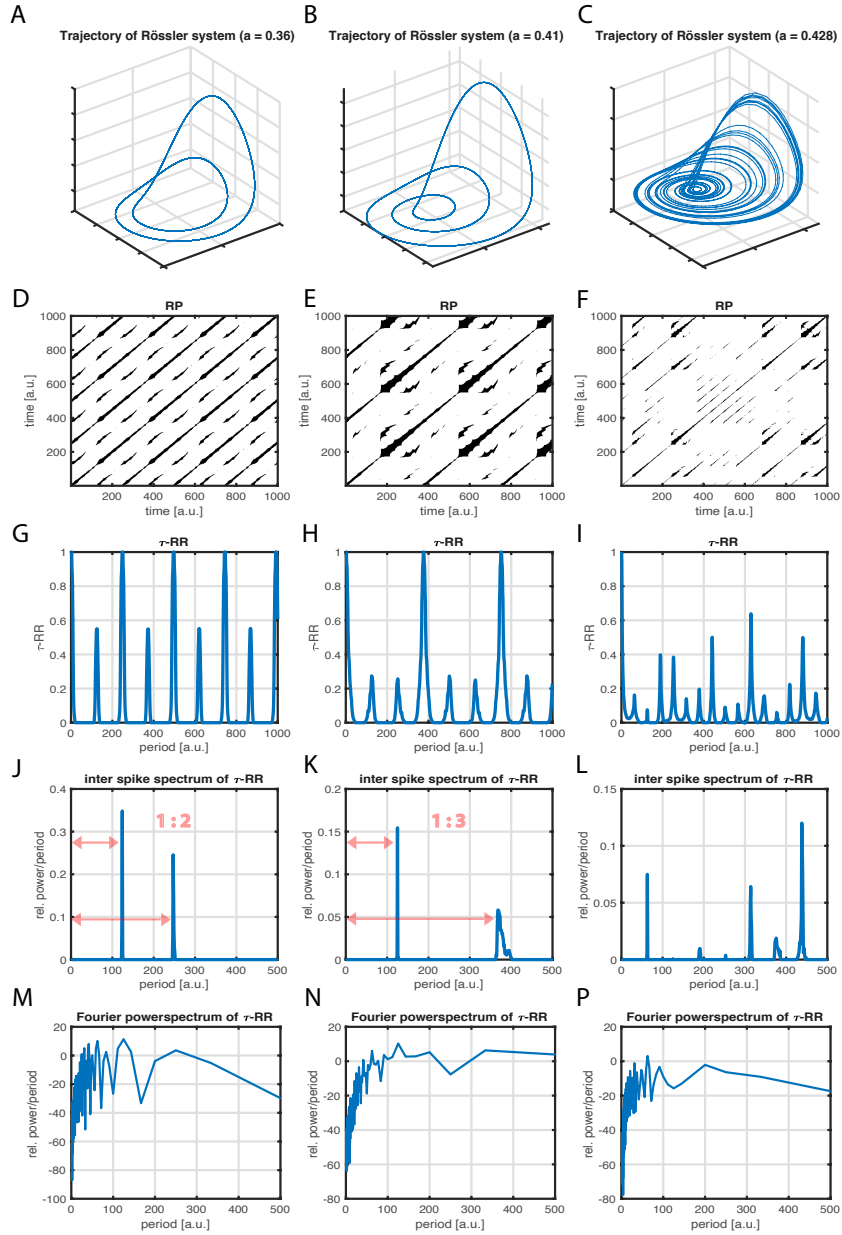


**Fig. 4** Inter spike spectra of the  $\tau$ -RR of the Rössler system in three different dynamical regimes with parameters  $b = 2$ ,  $c = 4$ . Trajectory of the system in **A** period-2 (parameter  $a = 0.36$ ), **B** in a period-3 (parameter  $a = 0.41$ ) and **C** in a chaotic regime (parameter  $a = 0.428$ ). **D, E, F** The corresponding RPs, obtained by using a recurrence threshold corresponding to a 10% global recurrence rate for D & E and 5% for F. **G, H, I**  $\tau$ -RR's of the shown RPs. **J, K, L** The proposed inter spike spectra of the  $\tau$ -RR's shown in panels G, H, I. Spectra were obtained with a LASSO regression and a regularization threshold corresponding to  $\rho = 0.95$  accordance of  $\tau$ -RR's and re-composed signals. The distance ratio of the peaks reflect the limit cycle dynamic. **M, N, P** Fourier power spectra of the  $\tau$ -RR's shown in panels G, H, I.

also robust to noise (see Fig. 6 in the Appendix). This is because the peaks of the  $\tau$ -RR are insensitive to noise. While the peak shape does change in the presence of noise, its position does not, and this is what the inter spike spectrum encrypts after all.

### 3.2 Bifurcations in the Logistic map

We consider the Logistic map  $x_{n+1} = r \cdot x_n (1 - x_n)$  for changing control parameter  $r$ . We vary  $r$  from  $r = 3.4$  to  $r = 4$  in steps of 0.001. For each setting of  $r$

- (1) a time series of length  $N = 201$  is computed with a random initial condition  $u_0 \in [0, 1]$ , neglecting the first 1,000 samples as transients,
- (2) 100 iterative Amplitude Adjusted Fourier Transform (iAAFT) surrogates [16, 17] are computed,
- (3) the time series and its iAAFT surrogates are embedded in a 2-dimensional state space using a time delay of unity,
- (4) from the 2-dimensional trajectories RPs, Eq. (1), are computed under a threshold  $\varepsilon = 0.05$ ,
- (5)  $\tau$ -RR, Eq. (2), is computed from the RP of the signal and from the RPs of the surrogates,
- (6) inter spike spectra are obtained from  $\tau$ -RR of the signal and from the  $\tau$ -RRs of the surrogates, see Section 2, and finally,
- (7) from the distribution of the surrogate inter spike spectra the 95<sup>th</sup> percentile is computed. The peaks of the inter spike spectrum of the signal which exceed this percentile are counted.

In this example, the according null hypothesis is that the data stems from a process which yields the same auto-correlation, hence the same Fourier powerspectrum, and the same amplitude distribution. We consider the number of significant peaks in the inter spike spectrum with respect to the control parameter in order to distinguish the corresponding dynamics (Fig. 5C). A correlation with the positive Lyapunov exponent (Fig. 5A) is discernible ( $\rho_{\text{Pearson}} = 0.72$ ). Moreover, this analysis can tackle period-doubling, since it “measures” the dominant cycles via the inter spike spectrum.

A less computationally intensive approach is to compute surrogates for the  $\tau$ -RR analytically, rather than computing a RP and its  $\tau$ -RR for each iAAFT surrogate of the time series. This translates into a null hypothesis that the  $\tau$ -RR and its corresponding inter spike spectrum stems from a RP of a random signal. In this case the probability of finding a black point in the RP can be obtained from a binomial distribution with probability parameter  $p$  set to the recurrence rate of the RP of the signal. This way 100 surrogate  $\tau$ -RRs are computed in step (5). The results are even slightly better compared to the ones obtained from the iAAFT surrogates (Fig. 5B,  $\rho_{\text{Pearson}} = 0.81$ ). The first period doubling at  $r \approx 3.458$  cannot be detected by any of the surrogates.

The described procedure does work well for map data, because most often the  $\tau$ -RR for those kind of data reveals a “spiky enough” nature. On the contrary, highly sampled (flow-) data often yield not as spiky  $\tau$ -RR’s and, thus, the number of significant peaks in the inter spike spectrum may not be sensitive enough to detect period-doubling bifurcations. Moreover the sensitivity of the inter spike spectrum to detect the regime shifts also depends on the critical regularization threshold. Nevertheless the according inter spike spectra is still revealing important information (Fig. 4) and practitioners can design appropriate quantifying statistics based on these spectra, which suit the research task.

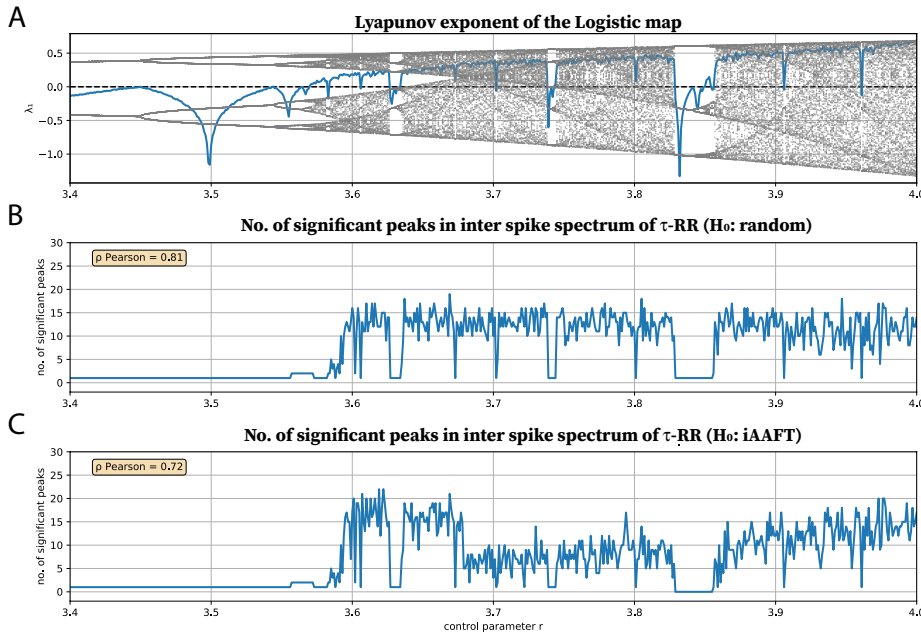


**Fig. 5** **A** Lyapunov exponent of the Logistic map as a function of the control parameter  $r$ . **B** Number of significant peaks ( $\alpha = 0.05$ ) in the inter spike spectrum of the  $\tau$ -RR and its Pearson correlation coefficient to the Lyapunov exponent shown in **A** (white noise surrogates). **C** Same as **B**, but for iterative Amplitude Adjusted Fourier Transform (iAAFT) surrogates [16, 17]. For obtaining the inter spike spectra we used a LASSO regression and a regularization threshold corresponding to  $\rho = 0.95$  accordance of  $\tau$ -RR's and recomposed signals.

### 3.3 Evolutionary spike spectrogram of CENOGRID isotope time series

## 4 Conclusion

A novel type of powerspectrum, the *inter spike spectrum*, has been proposed. The method decomposes any arbitrary signal into basis functions which consist of (lagged) Dirac combs (DC) of different inter-spike period. The loading for each period is obtained by a regularized regression, which promotes sparsity in its solution (we chose LASSO or a sequentially thresholded least squares regression STLS). Since there are  $M = \sum_{i=1}^{\lceil N/2 \rceil + 1} i$  basis functions for a signal of length  $N$  the regression can get computationally intensive for  $N > 1,000$ . When plotting the computed loadings as a function of the period (or frequency) the inter spike spectrum is obtained. This novel powerspectrum is superior to an ordinary FFT-based powerspectrum, when the signal has a spike-train-like appearance. Due to the sparse regression underlying the method, there is no unique inverse of the transformation and the regularization parameter plays a crucial role and determines the appearance of the obtained inter spike spectrum. Moreover, similar to the Nyquist frequency barrier in the Fourier Transform which sets a lower bound for the corresponding wave period, here the maximum considered inter spike period is bounded by  $T_{is}^{\max} = \lceil N/2 \rceil + 1$ .

The invention of the proposed method has been motivated by the idea of transforming  $\tau$ -recurrence rate signals ( $\tau$ -RR's) into their frequency domain. This general idea [19] allows for a frequency analysis of high dimensional systems, because the RP is a representation of

the system's state space trajectory. The  $\tau$ -RR of a recurrence plot (RP) usually has a spiky shape, especially for map-like data, and the inter spike spectrum can reliably reveal the system's dominant frequencies, which is not possible when Fourier transforming the  $\tau$ -RR or the underlying signal itself. Since the position of the peaks in the  $\tau$ -RR are not sensitive to noise, the corresponding inter spike spectrum also yields robust results in the presence of noise. We have successfully used the idea of transforming the  $\tau$ -RR for the detection of bifurcations in the Logistic map. By constructing appropriate surrogates of the inter spike spectra, and thus a null model, the number of significant peaks in the inter spike spectrum correlated well with the positive Lyapunov exponent. This measure was also able to resolve period-doubling bifurcations.

Here a quick summary of the other applications.

We could think of a broad range of applications of the proposed idea. The inter spike spectrum itself can serve as a valuable tool for the analysis of any sort of spike-train-like data. On the other hand, the inter spike spectrum of the  $\tau$ -RR of a signal can serve as a generalized, nonlinear frequency analysis tool for complex systems. When there is only a subset of state variables available, the state space has to be reconstructed as a pre-processing step. Recent findings [7, 8] show that this reconstruction process can be reliably automated and applied to multivariate data as well. This would allow for a “running window” approach, in order to detect transitions. Due to the mentioned computational constraints of our proposed method, a window size  $w \leq 1,000$  would possibly suffice for most data, especially when it is map-like, i.e., not highly sampled.

**Acknowledgements** This work has been financially supported by the German Research Foundation (DFG projects MA4759/8 and MA4759/9). All computations have been carried out in the Julia language and made use of the packages *DynamicalSystems.jl* [5] and *DifferentialEquations.jl* [13].

### Conflict of interest

The authors declare that they have no conflict of interest.

### A Inter spike spectra for noisy Rössler system

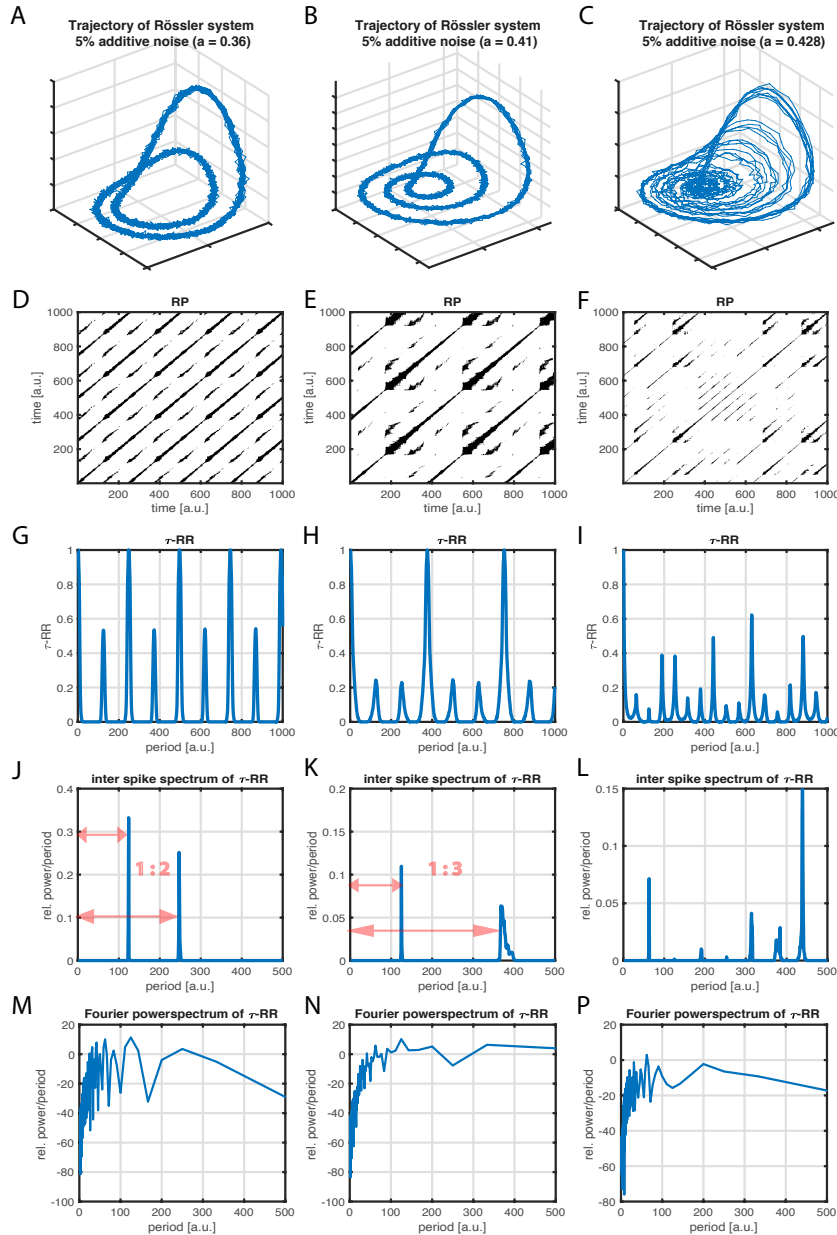


**Fig. 6** Same as in Fig. 4, but here with 5% additive Gaussian white noise. The appearance of the inter spike spectra in **J**, **K**, **L** and the Fourier spectra in **M**, **N**, **P** are unaffected by the additive noise noise.

## B Exemplary models

### B.1 Lorenz system

The classical Lorenz-63 system [9] is defined as

$$\begin{aligned}\dot{x} &= \sigma(y - x) \\ \dot{y} &= x(r - z) - y \\ \dot{z} &= xy - \beta z.\end{aligned}\tag{8}$$

For producing Fig. 1 we set the initial condition to  $u_0 = [0.0, 10.0, 0.0]$ , used a sampling time of  $\Delta t = 0.01$  and discarded the first 2,000 points of the integration as transients. The parameters have been set to  $\sigma = 10, \beta = 8/3, r = 28$  and we used a time series consisting of 6,000 samples.

### B.2 Rössler system

The Rössler system [14] is defined as

$$\begin{aligned}\dot{x} &= -y - z \\ \dot{y} &= x + ay \\ \dot{z} &= b + z(x - c).\end{aligned}\tag{9}$$

For producing Figs. 6, 4 the initial condition for producing panels A & B was set to  $u_0 = [.7, -1, 0.4]$  with a sampling time of  $dt = 0.05$  and in case of panel C  $u_0 = [-0.1242, -2.5415, 0.2772]$  with a sampling time of  $dt = 0.1$ . The first 5,000 samples were discarded as transients and trajectories of length  $N = 5,000$  were obtained from which we computed the RPs and the corresponding  $\tau$ -RR's. For the inter spike spectra only the first 1,000 values of the  $\tau$ -RR's were considered.

## References

1. Baptista MS, Ngamga EJ, Pinto PRF, Brito M, Kurths J (2010) Kolmogorov-Sinai entropy from recurrence times. Physics Letters A 374(9):1135–1140, DOI 10.1016/j.physleta.2009.12.057
2. Brunton SL, Kutz JN (2019) Data-Driven Science and Engineering: Machine Learning, Dynamical Systems, and Control. Cambridge University Press, DOI 10.1017/9781108380690
3. Brunton SL, Proctor JL, Kutz JN (2016) Discovering governing equations from data by sparse identification of nonlinear dynamical systems. Proceedings of the National Academy of Sciences 113(15):3932–3937, DOI 10.1073/pnas.1517384113, URL <https://www.pnas.org/doi/abs/10.1073/pnas.1517384113>, <https://www.pnas.org/doi/pdf/10.1073/pnas.1517384113>
4. Córdoba A (1989) Dirac combs. Letters in Mathematical Physics 17(3):191–196, DOI 10.1007/BF00401584, URL <https://doi.org/10.1007/BF00401584>
5. Datseris G (2018) Dynamicalsystems.jl: A julia software library for chaos and nonlinear dynamics. Journal of Open Source Software 3(23):598, DOI 10.21105/joss.00598, URL <https://doi.org/10.21105/joss.00598>
6. Kraemer KH, Marwan N (2019) Border effect corrections for diagonal line based recurrence quantification analysis measures. Physics Letters A 383(34):125977, DOI <https://doi.org/10.1016/j.physleta.2019.125977>, URL <http://www.sciencedirect.com/science/article/pii/S0375960119308448>
7. Kraemer KH, Datseris G, Kurths J, Kiss IZ, Ocampo-Espindola JL, Marwan N (2021) A unified and automated approach to attractor reconstruction. New Journal of Physics 23(3):033017, DOI 10.1088/1367-2630/abe336, URL <https://doi.org/10.1088/1367-2630/abe336>
8. Kraemer KH, Gelbrecht M, Pavithran I, Sujith RI, Marwan N (2022) Optimal state space reconstruction via monte carlo decision tree search. Nonlinear Dynamics 108(2):1525–1545, DOI 10.1007/s11071-022-07280-2, URL <https://doi.org/10.1007/s11071-022-07280-2>
9. Lorenz EN (1963) Deterministic nonperiodic flow. Journal of the Atmospheric Sciences 20(2):130–141, DOI 10.1175/1520-0469(1963)020<0130:DNF>2.0.CO;2
10. March TK, Chapman SC, Dendy RO (2005) Recurrence plot statistics and the effect of embedding. Physica D 200(1–2):171–184, DOI 10.1016/j.physd.2004.11.002

11. Marwan N, Kurths J (2002) Nonlinear analysis of bivariate data with cross recurrence plots. Physics Letters A 302(5–6):299–307, DOI 10.1016/S0375-9601(02)01170-2
12. Marwan N, Romano MC, Thiel M, Kurths J (2007) Recurrence Plots for the Analysis of Complex Systems. Physics Reports 438(5–6):237–329, DOI 10.1016/j.physrep.2006.11.001
13. Rackauckas C, Nie Q (2017) Differentialequations.jl—a performant and feature-rich ecosystem for solving differential equations in julia. Journal of Open Research Software 5(1)
14. Rössler O (1976) An equation for continuous chaos. Physics Letters A 57(5):397 – 398, DOI [https://doi.org/10.1016/0375-9601\(76\)90101-8](https://doi.org/10.1016/0375-9601(76)90101-8), URL <http://www.sciencedirect.com/science/article/pii/0375960176901018>
15. Schild D (1982) An efficient method for the fourier transform of a neuronal spike train. International Journal of Neuroscience 17(3):179–182, DOI 10.3109/00207458208985921, URL <https://doi.org/10.3109/00207458208985921>, <https://doi.org/10.3109/00207458208985921>
16. Schreiber T, Schmitz A (1996) Improved surrogate data for nonlinearity tests. Phys Rev Lett 77:635–638, DOI 10.1103/PhysRevLett.77.635, URL <https://link.aps.org/doi/10.1103/PhysRevLett.77.635>
17. Schreiber T, Schmitz A (2000) Surrogate time series. Physica D: Nonlinear Phenomena 142(3):346–382, DOI [https://doi.org/10.1016/S0167-2789\(00\)00043-9](https://doi.org/10.1016/S0167-2789(00)00043-9), URL <https://www.sciencedirect.com/science/article/pii/S0167278900000439>
18. Tibshirani R (1996) Regression shrinkage and selection via the lasso. Journal of the Royal Statistical Society: Series B (Methodological) 58(1):267–288, DOI <https://doi.org/10.1111/j.2517-6161.1996.tb02080.x>, URL <https://rss.onlinelibrary.wiley.com/doi/abs/10.1111/j.2517-6161.1996.tb02080.x>, <https://rss.onlinelibrary.wiley.com/doi/pdf/10.1111/j.2517-6161.1996.tb02080.x>
19. Zbilut JP, Marwan N (2008) The wiener–khinchin theorem and recurrence quantification. Physics Letters A 372(44):6622–6626, DOI <https://doi.org/10.1016/j.physleta.2008.09.027>, URL <https://www.sciencedirect.com/science/article/pii/S0375960108014102>